Variable Rotor-Resistance Control of Wind Turbine Generators

D.J. Burnham, *Student Member, IEEE,* S. Santoso, *Senior Member, IEEE,* E. Muljadi, *Senior Member, IEEE*

Abstract—By adding a variable external resistance to the rotor of an induction generator used in a wind turbine, it is possible to manipulate the torque-speed curve and control the output power. The hardware implementation is accomplished by a set of three-phase external resistors connected in series with the rotor windings. To vary the effective value of the external resistance, a three-phase diode bridge and a DC chopper with a variable duty cycle is commonly used. Thus, the wind turbine generator operates at variable slip above synchronous speed. This method is less flexible than a doubly-fed induction generator, but does not require the use of slip rings to access the rotor circuit. This paper describes the construction of a time-domain electromechanical model for a wind turbine. The model is used to evaluate control strategies for the output power based on stator power, the equivalent circuit, or aerodynamic torque. All are capable of maintaining a constant power beyond rated wind speed. The transient performance of the controllers is also compared and control based on the aerodynamic torque is found to be the fastest, albeit with high transient power deviations.

Index Terms—Wind power generation, induction generator, rotor resistance, variable speed wind turbine, wind turbine control

I. INTRODUCTION

Variable-speed wind turbines offer a number of control possibilities beyond those available with fixed-speed wind turbines. Two different types of variable speed turbines, both using wound-rotor induction generators, are common in to-day's market. Many manufacturers use doubly-fed induction generators (DFIGs), with the rotor circuit connected to the grid via a pair of inverters. In the United States, variable speed turbines based on modification of the generator torque-speed curve via an external resistance in the rotor circuit are also available [1]. In this case, the rotor resistor is mounted on the generator shaft and control signals are passed optically, eliminating the need for slip rings. A DC chopper circuit is used to pulse the resistor with a variable duty cycle, thus implementing a variable resistance with no moving parts. One disadvantage to this technique is the lack of control of reactive power consumption independent of the real power. Another is the high rotor losses, which increase with slip and limit the speed variation to approximately 10%. However, such a system may cost significantly less than a full DFIG system. While DFIG systems have been studied extensively [2], the discussion of the rotor resistance approach has been limited [3]-[4].

D.J. Burnham and S. Santoso are with the Department of Electrical and Computer Engineering, University of Texas at Austin, Austin, TX 78712.

E. Muljadi is with the National Renewable Energy Laboratory, Golden, CO 80401.

This paper presents several different methods for controlling the rotor resistance of a wind turbine induction generator to achieve a constant power output beyond the rated wind speed. The controllers considered will be simple, and will be evaluated based on their transient performance in addition to their ability to meet the constant power objective. The approach taken is the development of time-domain simulation models for a 1.5-MW turbine and several control systems. The model is used to evaluate the transient performance of the control systems. The results indicate that controlling for constant aerodynamic torque provides the fastest and most stable response, but at the expense of high transient-power overshoots and mechanical stress. Controlling directly for constant output power provides reasonable performance, but interestingly, little is gained by the addition of a lookup table to find the appropriate resistance for a given wind speed.

Sections II and III review the basic components of a wind turbine and the theory on which the variable rotor-resistance control is based. Section IV describes the time-domain electromechanical model that is used in Section V to evaluate controllers based on the generator output power, the generator equivalent circuit, and the aerodynamic torque. The evaluation is based on the transient performance of the controllers in response to sudden changes in wind speed.

II. WIND TURBINE COMPONENTS

A. Aerodynamics

For a wind turbine with blade radius R_{rot} operating in a wind with speed V_{wind}, the tip speed ratio λ is defined as the ratio of the blade tip linear speed to the wind speed, or

$$\lambda = \frac{R_{rot}\omega_{rot}}{V_{wind}}, \qquad (1)$$

where ω_{rot} is the rotor angular velocity. The power extracted from the wind is thus

$$P_{aero} = 0.5\rho C_p R_{rot}^2 V_{wind}^3 \qquad (2)$$

where ρ is the air density in kg/m^3 and C_p is the blade coefficient of performance, which depends on the blade aerodynamics. It is a function of both the blade pitch angle β and the tip speed ratio. Several empirical equations for estimating C_p are available in the literature [5]. However, if data is available for a specific blade geometry, it is more desirable to construct a lookup table that will provide C_p at any common pairing of β and λ.

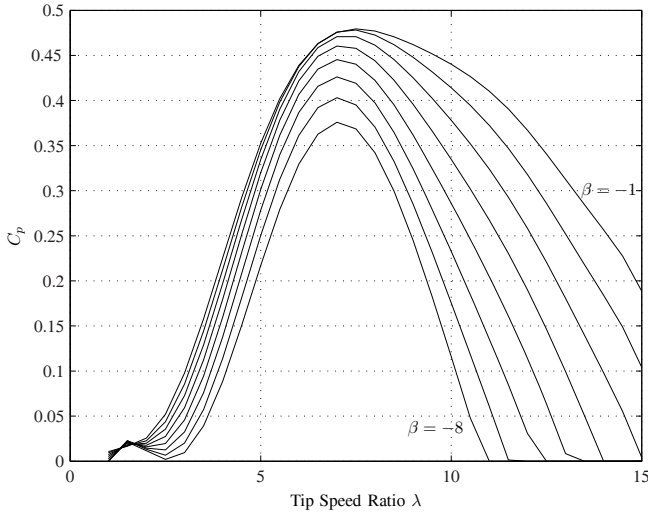A family of C_p curves is shown in Figure 1. Typical blade designs have the property that, for a given β, there will be

Fig. 1. C_p versus λ for $\beta = -8, -7, ..., -1$.
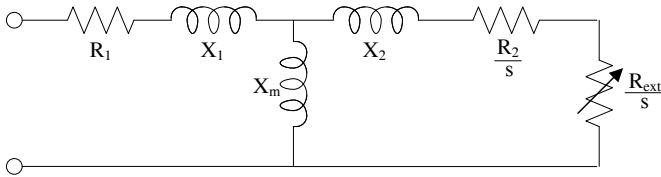

Fig. 2. Wound-rotor induction machine electrical model.

a single λ that maximizes C_p. However, a C_p below the maximum may be achieved at multiple values of λ.

B. Drive Train

Most utility-scale wind turbines use induction generators with two or three-pole pairs. The blades typically drive a low-speed shaft, which is connected to the high-speed generator shaft through a gearbox. However, the drive train can be modeled entirely on the high speed side of the gearbox, with values from the low speed shaft converted to the high speed side using the gear ratio. This results in an equivalent spring constant K and equivalent damping constant B.

To avoid confusion between the wind turbine rotor, consisting of the blades and hub, and the generator rotor, we will use the subscript "rot" to denote quantities at the wind turbine rotor and "gen" to denote quantities at the generator rotor.

The wind turbine blades naturally have a high rotational inertia, but the generator rotational inertia is also high enough that it cannot be neglected. Additionally, the need to reduce the nacelle weight typically results in shafts that are flexible to the point that their torsional spring constants cannot be neglected. Hence, a two-mass model is required to accurately depict the drive train [5].

C. Generator

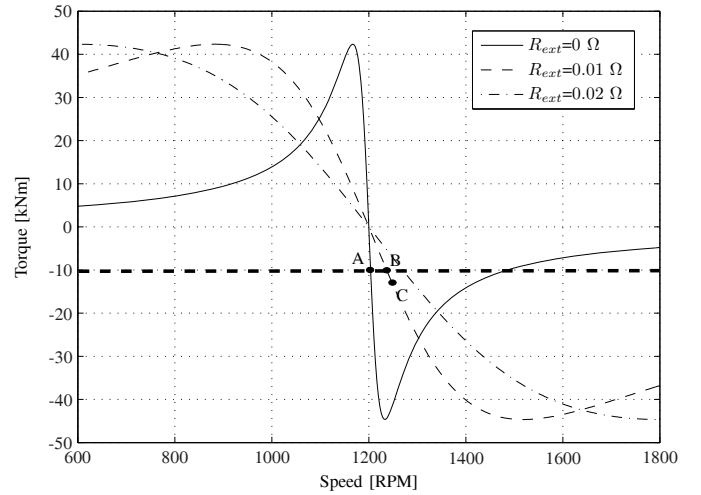Figure 2 shows the electrical model for a wound-rotor induction generator with a variable rotor-resistance R_{ext} and

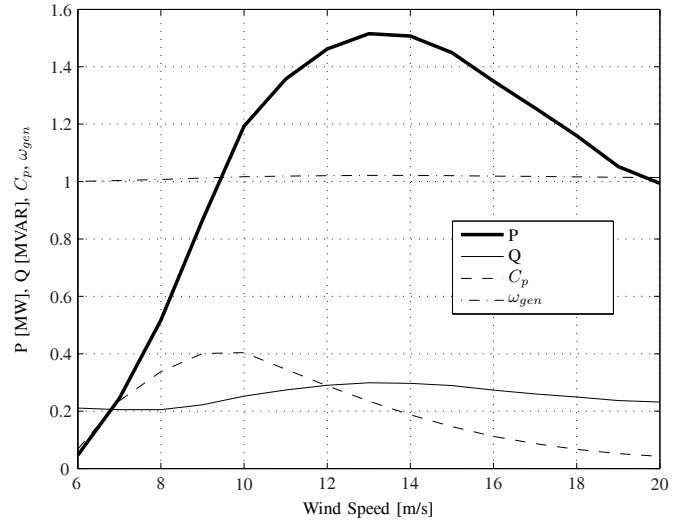Fig. 3. Induction machine torque-speed curves for different values of R_{ext}.

Fig. 4. Power P, reactive power Q, C_p, and ω_{gen} for a fixed-speed wind turbine. Positive Q is consumed by the generator.

an internal rotor-resistance R_2 [6]. The turns ratio between the stator and rotor has been eliminated by referring the rotor quantities to the stator side.

Torque-speed curves for a six-pole induction machine are shown in Figure 3, illustrating the dependence of the slope of the curve in the operating region on R_{ext}. The data for this machine is available in the appendix. In the generating region ($\omega_G > 1200$ rpm), a higher R_2 will cause the machine to operate at a higher speed for a given torque, illustrated by the line of constant torque and points A and B in Figure 3.

III. THEORY OF OPERATION

A typical wind turbine will have an output power that increases as V_{wind} increases from the cut-in wind speed to the rated wind speed. At the rated wind speed, the generator has reached rated power, and the electrical power must be held constant or reduced for further increases in wind speed. For a fixed speed turbine with a fixed blade pitch, the pitch must
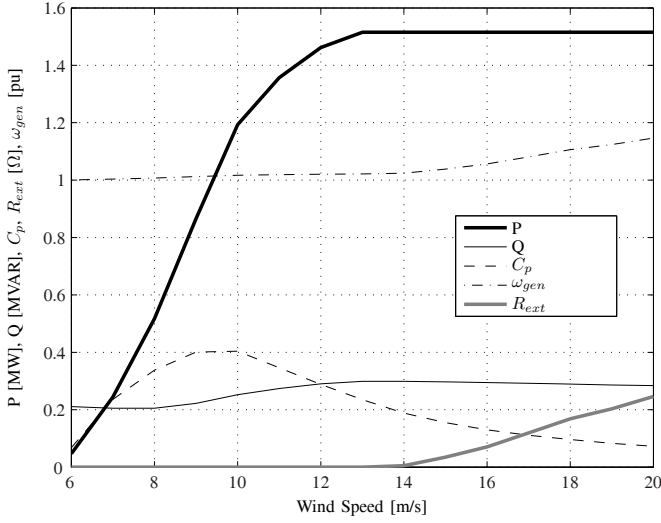
Fig. 5. Power P, reactive power Q, C_p, ω_{gen}, and R_{ext} for a variable-speed wind turbine with rotor-resistance control. Positive Q is consumed by the generator.

be selected so that higher wind speeds cause the blades to stall, reducing C_p and limiting the aerodynamic power. This results in a power curve that decreases between the rated and cut-out wind speeds. One such power curve, for a 1.5-MW turbine with a rated wind speed of 13 m/s, is show in Figure 4. In fact, C_p peaks at a wind speed below rated and further increases in power are the result of the fact that P_{aero} increases with the cube of the wind speed.

By considering (1) and noting that beyond rated wind speed the wind speed increases while the generator speed decreases, it should be clear that λ decreases with increasing wind speed. The operating point at a given β has thus moved to the left along the curves in Figure 1. By increasing λ, it should be possible to increase C_p and obtain a greater power extraction from the wind.

One option for increasing lambda is to increase the generator speed. This is accomplished by introducing the external rotor resistance R_{ext}, increasing the speed at which the generator will operate for a given torque. Visually, this moves the operating point in Figure 3 from point A to point B. The additional losses in the rotor resistor account for most of the additional mechanical power extracted in this step. However, operating at a higher ω_{gen} also increases λ, increasing the aerodynamic torque, and resulting in steady state operation at point C in Figure 3. This increases the electrical power output of the generator.

With power electronics to continually adjust R_{ext} to maintain a constant output power, the curves shown in Figure 5 result. Since the generator speed now varies by approximately 12%, this arrangement is considered to be a variable-slip wind turbine.

The value of R_{ext} needed to maintain a constant generator power is also shown in Figure 5. At the cut-out wind speed of 20 m/s, the losses in the rotor circuit are 192 kW. In reality, the heating due to these losses is undesirable, and the blade pitch should eventually be adjusted to maintain rated power
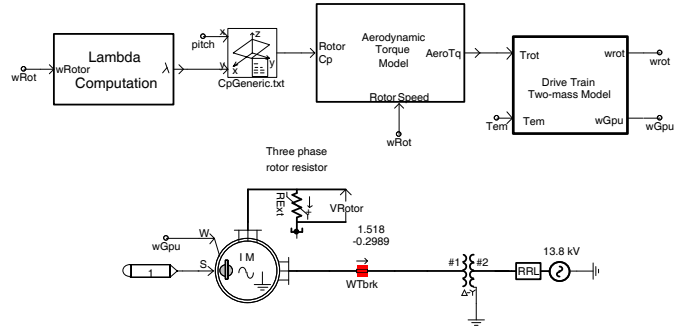

Fig. 6. PSCAD model for a 1.5 MW wind turbine.

and reduce R_{ext} to zero. The rotor-resistance control system can then be used to maintain a constant output power for small deviations about a steady-state wind speed, reducing the additional resistance required and the associated losses. Since the variable R_{ext} can be implemented electronically, it is possible to obtain a much faster response to wind speed variations than would be possible by pitch control alone. It is also possible to reduce the wear on the pitch control motors by only using the pitch system to compensate for wind speed variations larger than a particular threshold.

It must be noted that the reactive power consumed by the induction generator cannot be controlled independent of the real power. External power-factor correction is still required. The reactive power consumed in the region beyond rated wind speed varies less with the variable speed turbine than with the fixed speed turbine, and may reduce the number of switching events if a switched capacitor bank is used.

IV. TIME-DOMAIN ELECTROMECHANICAL SIMULATION

A model of a 1.5-MW fixed-pitch wind turbine with a variable rotor resistance has been implemented in PSCAD/EMTDC software, following the approach of [7]. The tip speed ratio is first computed using (1), and a lookup table is used to determine C_p. The two-mass model for the drive train solves the differential equation pair

$$J_{rot}\ddot{\theta}_{rot} + B(\omega_{rot} - \omega_{gen}) + K(\theta_{rot} - \theta_{gen}) = \Gamma_{rot} \quad (3)$$

$$J_{gen}\ddot{\theta}_{gen} + B(\omega_{gen} - \omega_{rot}) + K(\theta_{gen} - \theta_{rot}) = -\Gamma_{gen} \quad (4)$$

Additional model parameters are given in the appendix. The power curves in Figures 4 and 5 were generated using this model.

For this simulation, the value of R_{ext} is adjusted directly by the controller. However, in practice a variable resistance would be implemented using a chopper circuit, such as those found in [4] or [8], with the controller specifying the duty ratio. The switching frequency of such a circuit would necessitate a small simulation time-step, and since its response can be expected to be much faster than the rest of the system, it is valid to use a simple variable resistor instead, allowing for a more efficient simulation. It should be noted that the switching frequency will introduce high frequency harmonics and, depending on the implementation, harmonics near the rotor slip frequency [8]. These harmonics are not captured by this model.
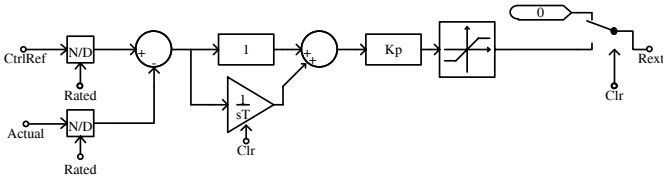
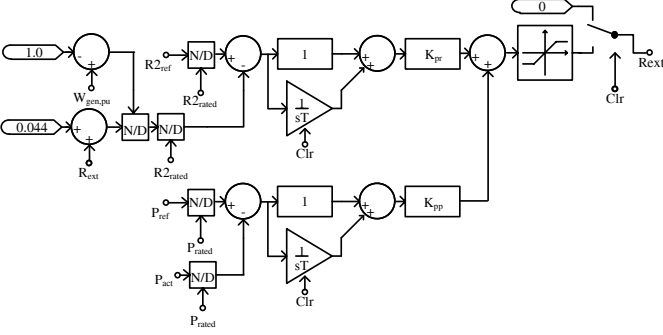Fig. 7. Power controller with per-unitization of inputs and output limiter.

Fig. 8. Control for $\frac{R_2 + R_{ext}}{s}$ and output power.
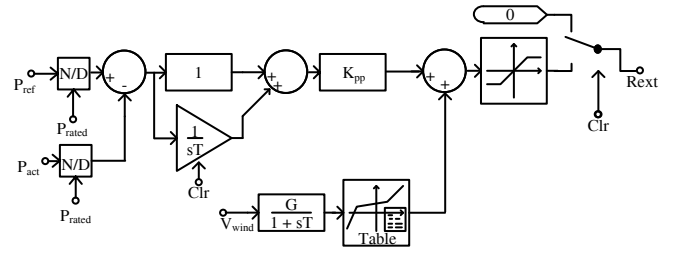

Fig. 9. Power control with lookup table.

and

$$T_i = \frac{1}{1.2} T_{cr}. \qquad (6)$$

All the controllers presented here were tested to ensure their stability at all wind speeds between rated and cut out. The controller transient performance, however, is presented only for step changes in wind speed from 17 m/s to 18 m/s, and 18 m/s to 17 m/s. While a true wind-speed step is not realistic, the use of a step input to characterize control systems is common, and the step can be considered an approximation of an extreme wind gust. To simulate the use of pitch control, the blade pitch was adjusted to achieve rated power output at 17 m/s wind speed before the wind speed step was applied. Thus, the initial value of R_{ext} is zero.

A. Output Power

The most obvious control scheme applies a proportional integral (PI) controller to the generator output-power error, as shown in Figure 7.

One difficulty in implementing such a controller is the fact that the large rotation inertia of the wind turbine blades and low shaft stiffness make the turbine output power slow to respond to changes in the generator rotor resistance. This forces the use of a relatively slow PI controller. The induction generator is also highly nonlinear, and thus, difficult to control.

The power controller has reasonable performance with $T_i = 0.2$ s and $K_p = 0.1$. The addition of a derivative term was found to improve the speed of the response to a step input, but resulted in large overshoots and extended oscillations. Figures 10 and 11 show the response of the turbine output power to a step change in wind speed (several other control options are also shown). In response to a wind speed change from 17 m/s to 18 m/s, the output power drops 18% to 1.23 MW, with a settling time of 3 s until the power returns to within 5% of rated. The overshoot in response to a wind speed drop from 18 m/s to 17 m/s is a rise to 1.72 MW (14.6%), with a settling time of 3.3 s. The asymmetry in the responses is due to the nonlinear nature of both the C_p curve and the induction generator.

B. Lookup Table

Since wind turbines almost always include equipment for measuring wind speed, it is possible to feed this information through a lookup table and obtain a value for R_{ext} that may be further refined by a controller, as shown in Figure 9. The addition of a lookup table to the controller described above

The generator selected for this simulation had a slip at rated power of approximately 2%. While this may be high when compared to typical induction motors, it simplifies the design of the control system since the sensitivity to small changes in R_{ext} is reduced when compared to a generator with a lower rated slip.

V. CONTROL

A controller is required to adjust the rotor resistance to maintain constant power beyond the rated wind speed. Several different control options are possible, and all have been simulated using the PSCAD model. It is important that the controller be disabled at and below the rated wind speed, since the output power in this region cannot be increased and the additional R_{ext} will result in increased rotor losses. It is also important to ensure that the integral term in the controller is reset to zero when the controller is disabled. Otherwise, it is likely to saturate and cause large overshoots when the controller is enabled. Finally, it is important to limit the value of R_{ext} to reasonable values. Since the value of λ that results in a particular power output may be non-unique, it is important to set an upper limit on the value of R_{ext}, preventing the simulation from reaching an equilibrium at high rotational velocity. For this simulation, a maximum limit of 0.3 Ω was used.

To keep the reference, error, and feedback signals near unity, per-unit values are used in the control system.

Because the generator and C_p models are highly nonlinear the controller parameters are determined by tuning rather than via analytical methods. In each case we employed the Ziegler-Nichols tuning rules [9]. Beginning with only proportional control, the gain K_p was increased until the onset of sustained oscillations with period T_{cr} at K_{cr}. The PI controller was then tuned manually, starting with
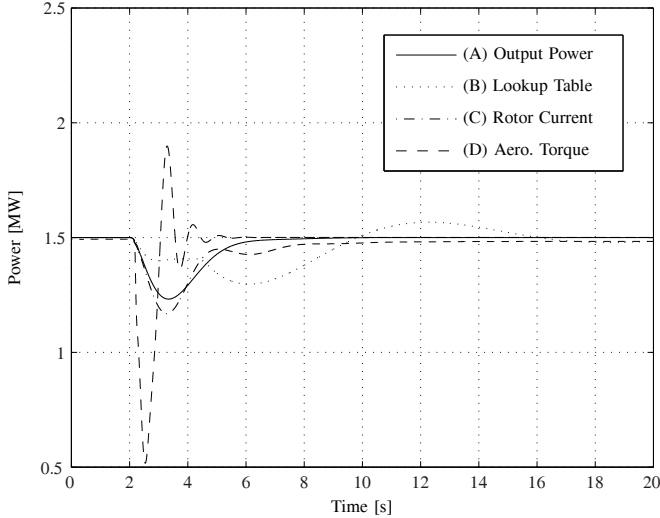
$$K_p = 0.45 K_{cr} \qquad (5)$$

Fig. 10. Response to a wind speed step from 17 to 18 m/s, various controllers.
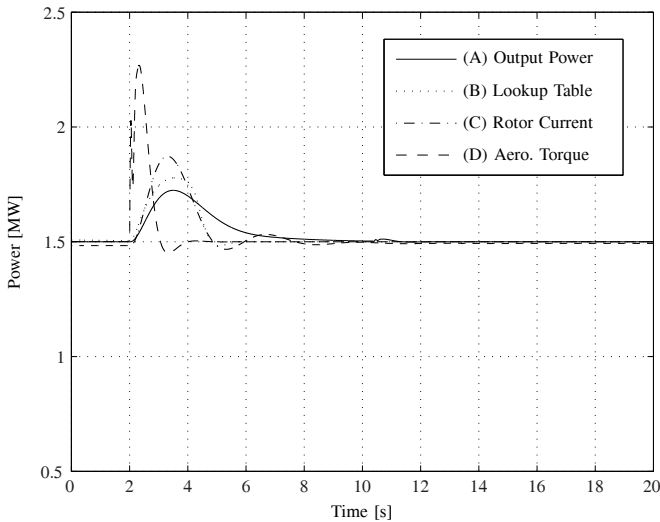

Fig. 11. Response to a wind speed step from 18 to 17 m/s, various controllers.

results in a response to the wind-speed step increase with a power drop to 1.3 MW, with a much longer settling time of 6.5 s. The response to a step decrease in wind speed is a power peak at 1.77 MW and a settling time of 2.5 s. It should be clear that the transient performance of this controller is worse than the PI controller alone. Because of the delay introduced by filtering the wind speed input to the lookup table, the PI controller has already begun to adjust R_{ext} when the lookup table reacts. The output from the PI controller must then re-adjust, extending the time needed to reach steady state.

C. Constant Rotor Current

As shown in the WRIM electrical model (Figure 2), all of the effects of speed changes are concentrated in the

$$\frac{R_2 + R_{ext}}{s} \tag{7}$$

component. If R_{ext} is adjusted such that the total value of this term remains constant, the equivalent circuit will be

unchanged. While it may be difficult in practice to measure R_2 and R_{ext}, the same result may be achieved by controlling for a constant rotor current I_r, which is relatively easy to measure.

Unfortunately, ensuring that the rotor current remains constant is not sufficient to ensure constant output power, but is capable of reducing the generator power variation to a few percent. In practice, this variation should be tolerable.

Using this control system, the response to a wind-speed step increase is an initial power drop to 1.18 MW (21%), and a settling time of 4.6 s. The power peaks at 1.87 MW (25%) in response to a wind-speed step decrease, with a settling time of 4.5 s. As illustrated in Figures 10 and 11, the performance of this controller is comparable to the output power controller described above.

D. Aerodynamic Torque

Neglecting losses other than those in the rotor resistance, the power balance for the wind turbine operating in steady state is

$$P_{aero} - P_R = P_G \tag{8}$$

where P_R is the losses in the rotor resistance, and P_G is the output power. The P_{aero} term may be rewritten, giving

$$\Gamma_{aero}\omega_{rot} - P_R = P_G, \tag{9}$$

where Γ_{aero} is the aerodynamic torque. If a controller is used to hold Γ_{aero} constant, the losses in the rotor will exactly compensate for the power resulting from the increase in ω_{rot}, and P_G will be fixed.

The control topology for constant aerodynamic torque is identical to the one used for constant output power and shown in Figure 7. It was found that $K_p = 5$ and $T_i = 0.2$ s gave a very good settling time in response to the wind speed steps, as shown in Figures 10 and 11. For the wind-speed step increase, the settling time is reduced to 1.8 s, but the power dropped to 0.5 MW en-route, a decrease of 67%. The response to the wind speed drop was an overshoot to 2.25 MW (83%), and settling time of 0.9 s.

The improved performance with respect to settling time in this case is largely the result of the increased gain term K_p. When controlling based on the aerodynamic torque, the system appears more linear, and the gain term may be set to a higher value without sacrificing stability.

In reality, the large power overshoots in response to wind speed steps are undesirable, and result in high torques on the drive train. However, the fact that it was possible to generate such a controller while maintaining system stability shows that control based on the aerodynamic torque has the potential to be quite robust. One important limitation is that in practice the measurement of the aerodynamic torque is difficult. An alternative is to measure or estimate the generator torque which, in steady state, will be equal to the aerodynamic torque.

VI. CONCLUSION

Using a variable resistor in the rotor circuit, it is possible to control the real power output of a wind turbine using a

wound-rotor induction machine. In particular, the output power can be held constant between the rated and cut-out wind speeds. When combined with pitch control, this can reduce the variability and increase the power output of a wind turbine. The increased aerodynamic power capture compensates for the additional losses in the additional rotor resistance.

Several different approaches are possible when designing a controller for the rotor resistance. Of the control strategies presented here, controlling directly for constant output power or constant aerodynamic torque are the most desirable. The output power controller provides reasonable performance, and is quite simple to implement and tune. The aerodynamic torque controller can be more responsive without introducing instabilities, but may result in high power and torque excursions. It may also be more difficult to accurately measure the aerodynamic torque.

APPENDIX
WIND TURBINE DATA

TABLE I
GENERATOR

Parameter	Variable	Value
Rated Power	P_{rated}	1.8 MW
Rated Line Voltage	V_{rated}	690 V
Rated Frequency	f	60 Hz
Stator Resistance	R_1	0.00125 Ω
Stator Leakage Reactance	X_1	0.0212 Ω
Rotor Resistance	R_2	0.0044 Ω
Rotor Leakage Reactance	X_2	0.0126 Ω
Magnetizing Reactance	X_m	1.807 Ω
Stator-Rotor Turns Ratio		0.379
Number of Poles	p	6

The rotor values in Table I have been referred to the stator side using the stator-rotor turns ratio.

TABLE II
DRIVE TRAIN

Parameter	Variable	Value
Gearbox Ratio	g	70.2
Generator Inertia	J_{gen}	90 kgm^2
Rotor Inertia	J_{rot}	5×10^6 kgm^2
Equivalent Spring Constant	K	19709 Nm/rad
Equivalent Damping	B	33.2 Nms/rad

In Table II, K represents the combination of the low-speed and high-speed shaft spring constants. B represents the combination of the low-speed shaft and high-speed shaft damping coefficients.

ACKNOWLEDGMENT

REFERENCES

[1] *Vestas V80-1.8 MW Datasheet*, Portland, OR: Vestas Americas, 2006.
[2] R. C. Bansal, T. S. Bhatti, and D. P. Kothari, D.P., "Bibliography on the application of induction generators in nonconventional energy systems," *Energy Conversion, IEEE Transactions on*, vol.18, no.3, pp. 433-439, Sept. 2003
[3] C. Velayudhan and J. H. Bundell, "A new automatic generation controller for a wind-driven slip-ring induction generator," *Proceedings of the IEEE*, vol.72, no.9, pp. 1226-1229, Sept. 1984
[4] C. V. Nayar and J. H. Bundell, "Output Power Controller for a Wind-Driven Induction Generator," *Aerospace and Electronic Systems, IEEE Transactions on*, vol. AES-23, no.3, pp.388-401, May 1987.
[5] H. Knudsen, J. N. Nielsen, "Introduction to the Modelling of Wind Turbines," in *Wind Power in Power Systems*, T. Ackermann, Ed. Chichester, West Sussex, England: John Wiley & Sons, 2005.
[6] S. J. Chapman, *Electric Machinery Fundamentals*, 3rd ed. Boston: McGraw-Hill, 1999.
[7] S. Santoso and H. T. Le, "Fundamental time-domain wind turbine models for wind power studies", *Renewable Energy*, vol.32, no.14, pp. 2436-3452, Nov. 2007.
[8] S. Heier, *Grid Integration of Wind Energy Conversion Systems*, 2nd ed. Chichester, West Sussex, England: John Wiley & Sons, 2006.
[9] K. Ogata, *Modern Control Engineering*, 3rd ed. Upper Saddle River, NJ: Prentice-Hall, 1997.

David J. Burnham (S'06) received a Bachelor of Arts in Engineering Sciences and a Bachelor of Engineering from Dartmouth College in Hanover, NH in 2006 and 2007, respectively. He is currently working towards the Master of Science degree in the Department of Electrical and Computer Engineering at the University of Texas at Austin. His current research interests include computer and experimental modeling of wind turbines and control systems.

Surya Santoso (S'95–M'96–SM'02) received the B.S. degree in electrical engineering from Satya Wacana Christian University, Indonesia, and the M.S. and Ph.D. degrees from the University of Texas at Austin, Austin, in 1992, 1994, and 1996, respectively, all in electrical engineering.

From 1997 to 2003, he was a Senior Power Systems/Consulting Engineer with Electrotek Concepts, Knoxville, TN. Since 2003, he has been an Assistant Professor in the Department of Electrical and Computer Engineering, University of Texas at Austin. His current research interests include power system analysis, modeling, and simulation, and impacts of wind power on power systems. He is the coauthor of Electrical Power Systems Quality (McGraw-Hill, 2002).

Dr. Santoso is the member of the IEEE PES Power Systems Analysis, Computing, and Economics Committee. He is a Chair of a task force on Intelligent System Applications to Data Mining and Data Analysis.

Eduard Muljadi received his Ph. D. (in Electrical Engineering) from the University of Wisconsin, Madison. From 1988 to 1992, he taught at California State University, Fresno, CA. In June 1992, he joined the National Renewable Energy Laboratory in Golden, Colorado. His current research interests are in the fields of electric machines, power electronics, and power systems in general with emphasis on renewable energy applications. He is member of Eta Kappa Nu, Sigma Xi and a Senior Member of IEEE. He is involved in the activities of the IEEE Industry Application Society (IAS) and Power Engineering Society (PES). He is currently a member of Industrial Drives Committee, Electric Machines Committee, and Industrial Power Converter Committee of the IAS, and a member of the Working Group on Renewable Technologies and the Dynamic Performance of Wind Task Force of the PES. He holds two patents in power conversion for renewable energy.